Appendix: Supplementary tables and figures

Supplementary Table 1: Pairwise Pearson correlation coefficients for amphibian diversity metrics.

	PE	EDGE
PD	0.60	0.91
PE		0.47

Supplementary Table 2: Pairwise Pearson correlation coefficients for mammal diversity metrics.

	PE	EDGE
PD	0.65	0.95
PE		0.65

Supplementary Table 3: Pairwise Pearson correlation coefficients for avian diversity metrics.

	PE	EDGE
PD	0.73	0.96
PE		0.73

Supplementary Table 4: Pairwise Pearson correlation coefficients for angiosperm diversity metrics. EDGE was not computed for angiosperms because of lack of information on IUCN threat categories.

	PE	ED
PD	0.86	0.97
PE		0.86

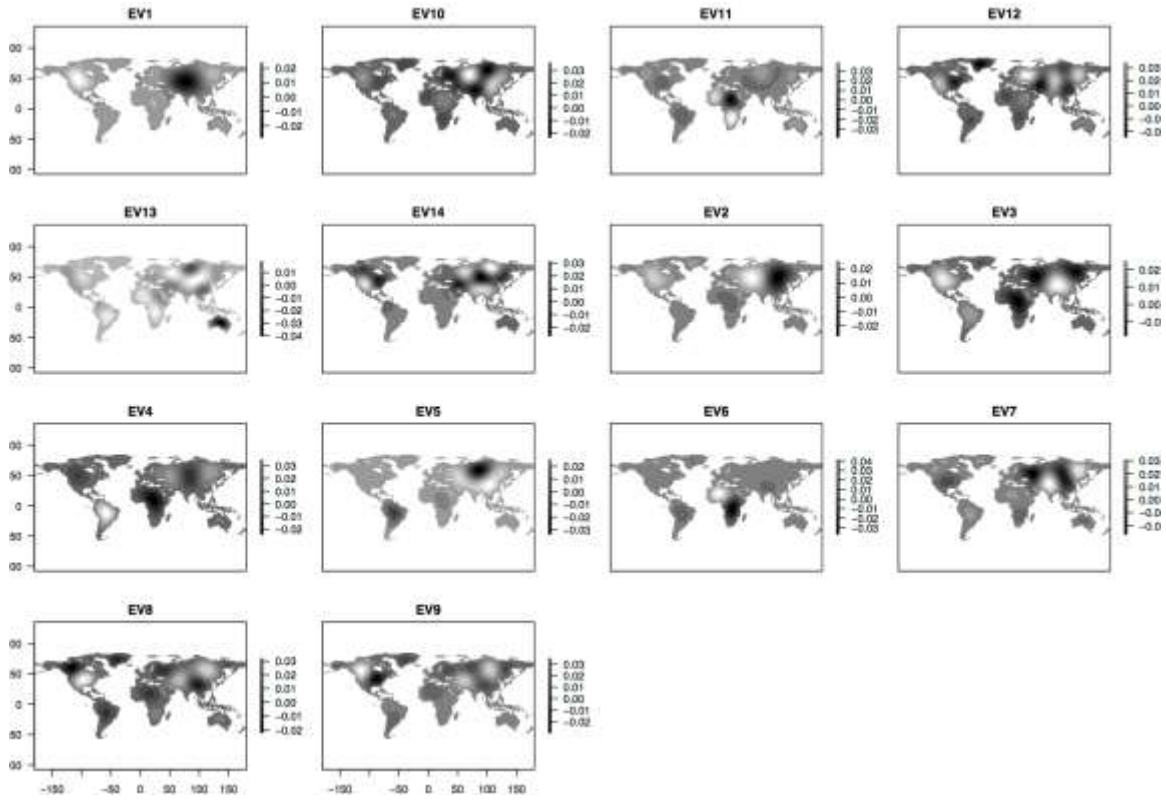

Fig. S1. The geographic patterns of the first 14 spatial filters showing the geographical connectivity among grid cells covering terrestrial areas on Earth except Antarctica at a spatial grain of 1° × 1°. Darker areas indicate regions of low numerical values of the eigenvectors and lighter areas indicate increasing values of the eigenvectors.

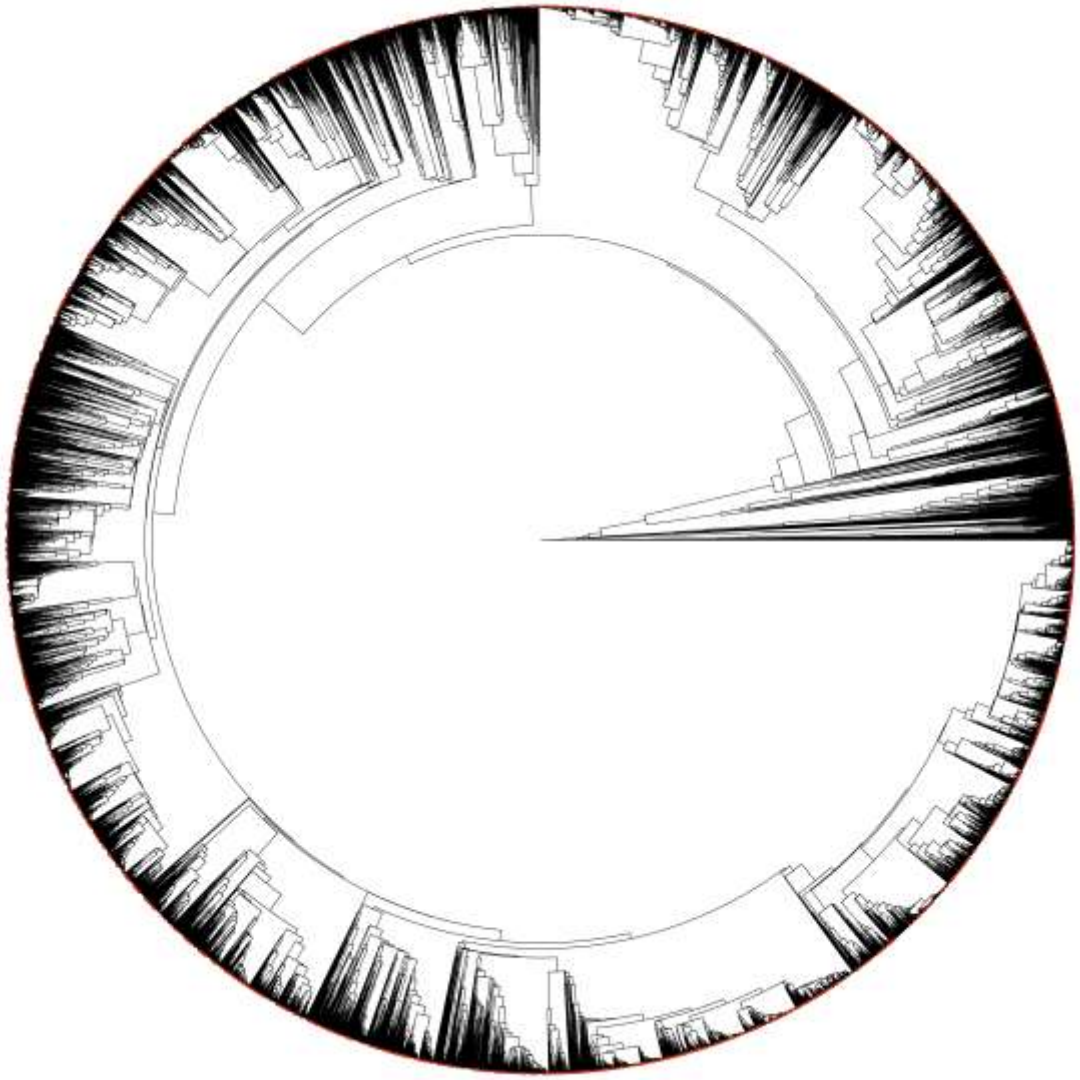

Fig. S2. Dated molecular phylogeny of 8179 angiosperm genera adapted from Zanne et al. (2013), with permission. Phylogenetic positions of missing taxa are indicated in red.

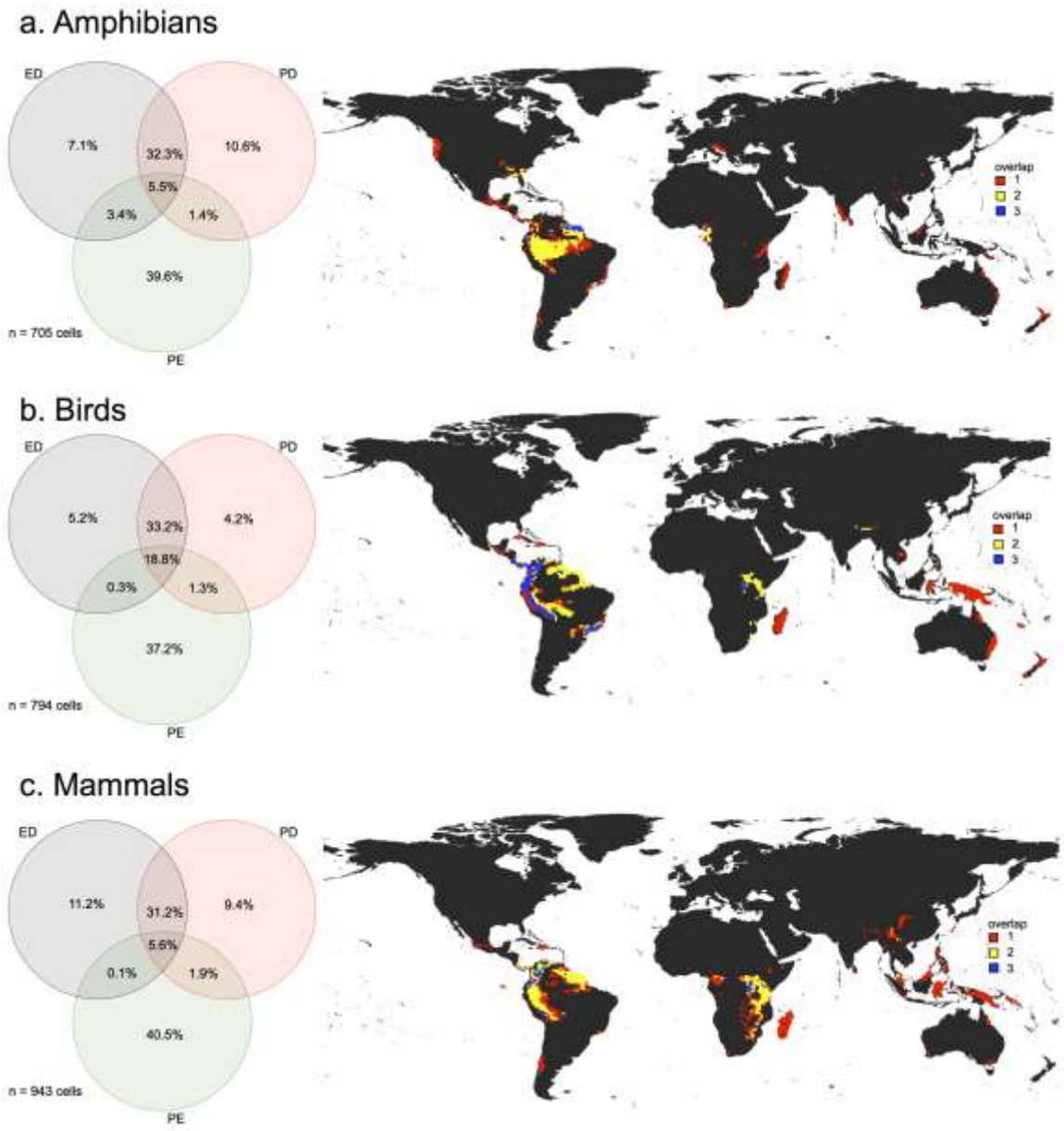

Fig. S3. Genus-level spatial congruence among three types of phylodiversity hotspots for (a) amphibians, (b) mammals, and (c) birds. Values in Venn diagrams are percentages of the total number of hotspot grid cells (top 2.5% quantiles) covered by all metrics combined together, with the middle values representing grid cells shared by all three metrics (also represented geographically in blue), and the others are grid cells unique to each metric (indicated geographically in red).

Fig. S4. Biodiversity hotspots from species-level metrics within equal-area grid cells (ca. 110 km × 110 km grids). The hotspots are a combination of the top 2.5% quantiles for each species-level diversity metric (global endangerment, species richness and species endemism) for each taxonomic group.

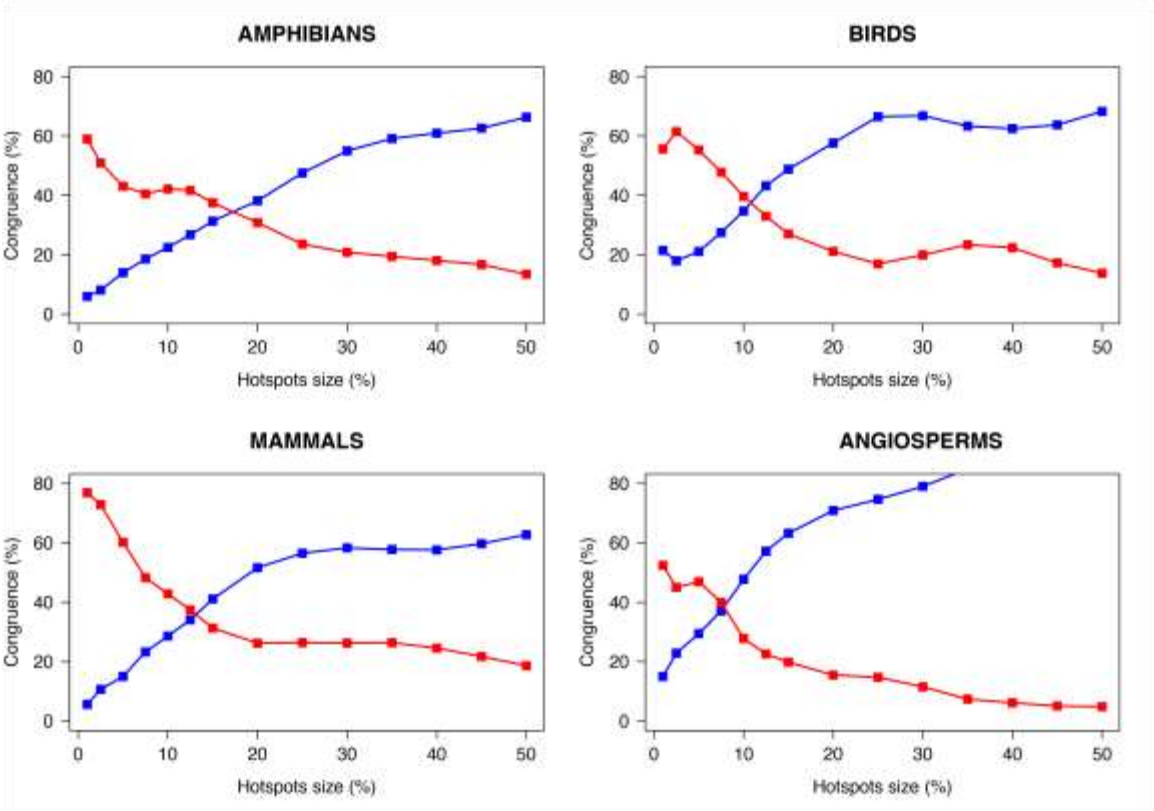

Fig. S5. Relationships between hotspots size and congruence among the phylodiversity hotspots for each taxonomic group; (a) amphibians, (b) birds, (c) mammals, and (d) angiosperms. The blue lines indicate spatial matches among the three types of phylodiversity metrics; the red lines correspond to the percentage of cells unique to individual phylodiversity metrics.

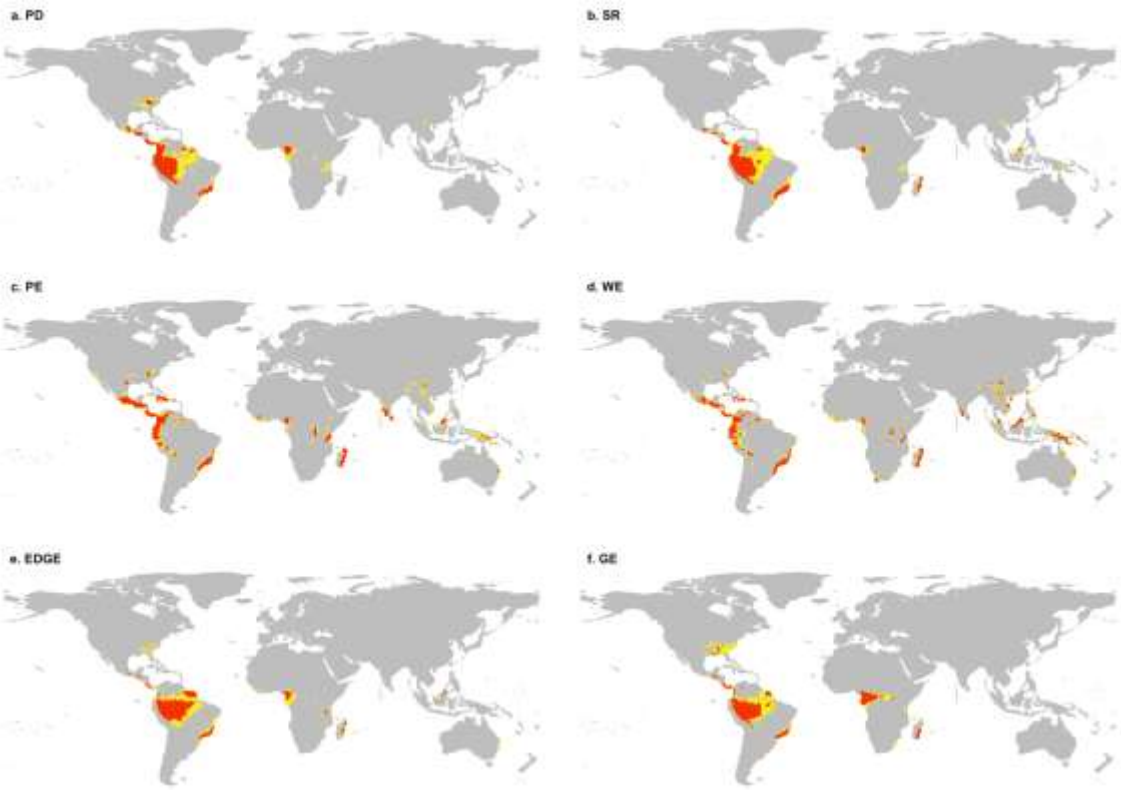

Fig. S6. Hotspots of amphibian diversity for phylogenetic indices versus species-level metrics; (a) phylogenetic diversity, (b) species richness, (c) phylogenetic endemism, (d) species weighted endemism, (e) summed EDGE and (f) summed GE. The richest 2.5% hotspot cells are shown in red, and the 5.0% hotspots in yellow.

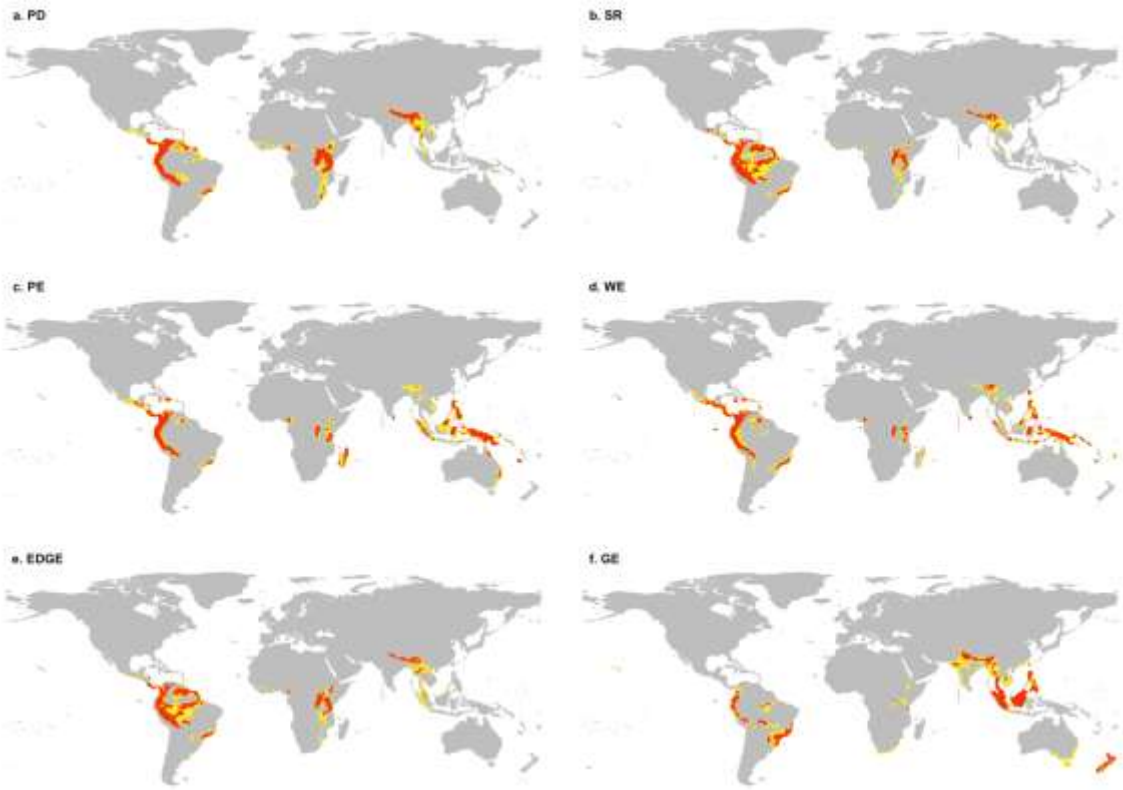

Fig. S7. Hotspots of bird diversity for phylogenetic indices versus species-level metrics; (a) phylogenetic diversity, (b) species richness, (c) phylogenetic endemism, (d) species weighted endemism, (e) summed EDGE and (f) summed GE. The richest 2.5% hotspot cells are shown in red, and the 5.0% hotspots in yellow.

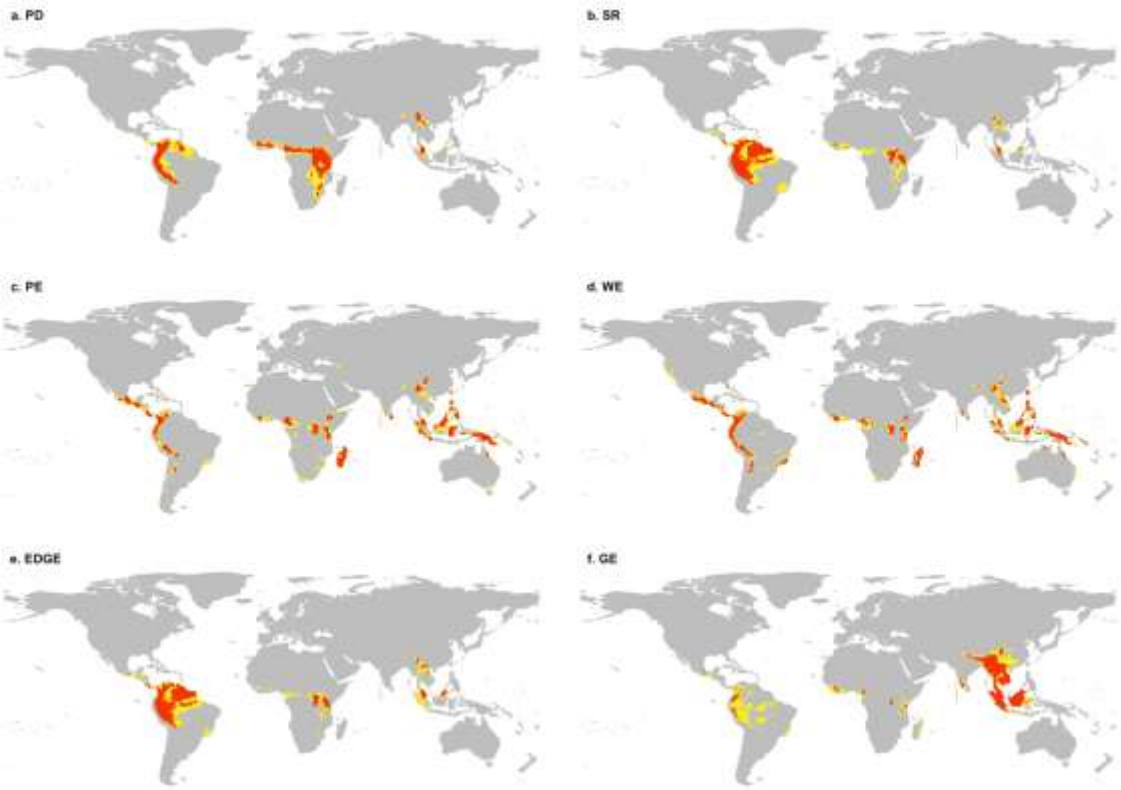

Fig. S8. Hotspots of mammalian diversity for phylogenetic indices versus species-level metrics; (a) phylogenetic diversity, (b) species richness, (c) phylogenetic endemism, (d) species weighted endemism, (e) summed EDGE and (f) summed GE. The richest 2.5% hotspot cells are shown in red, and the 5.0% hotspots in yellow.

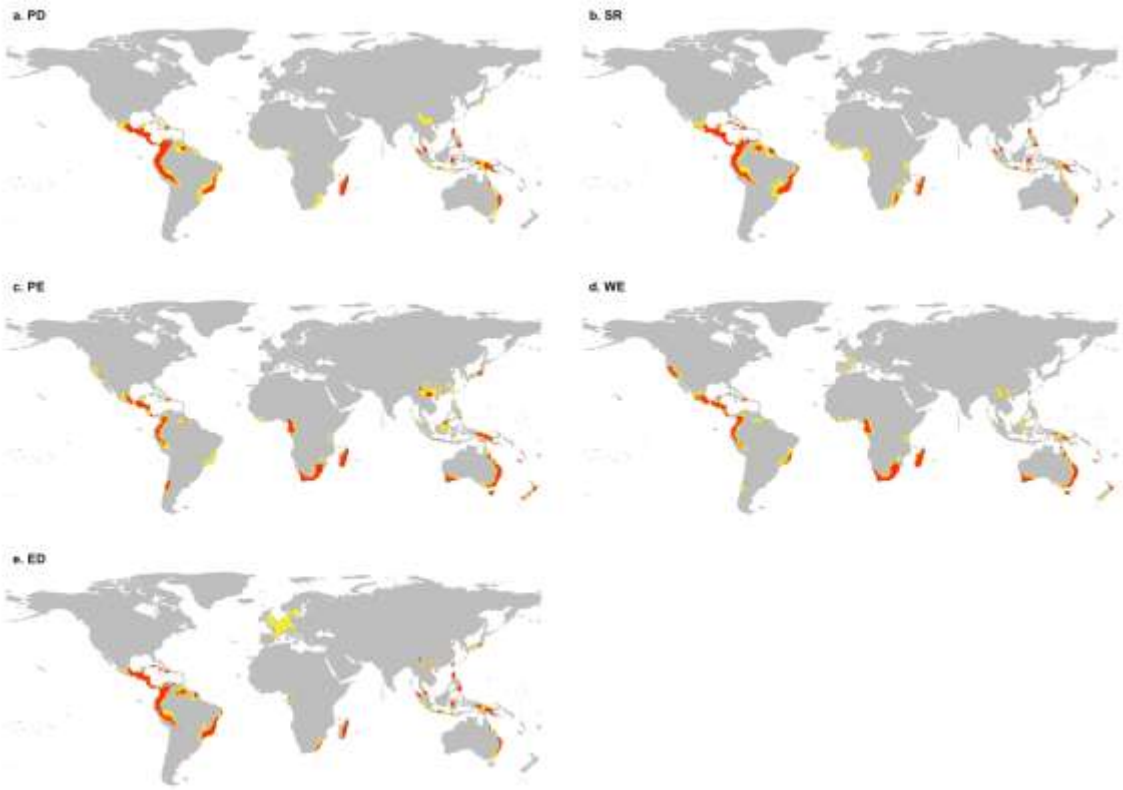

Fig. S9. Hotspots of angiosperm diversity for phylogenetic indices versus species-level metrics; (a) phylogenetic diversity, (b) species richness, (c) phylogenetic endemism, (d) species weighted endemism, and (e) summed ED. The richest 2.5% hotspot cells are shown in red, and the 5.0% hotspots in yellow. EDGE was not computed for angiosperms because of lack of information on IUCN threat categories.

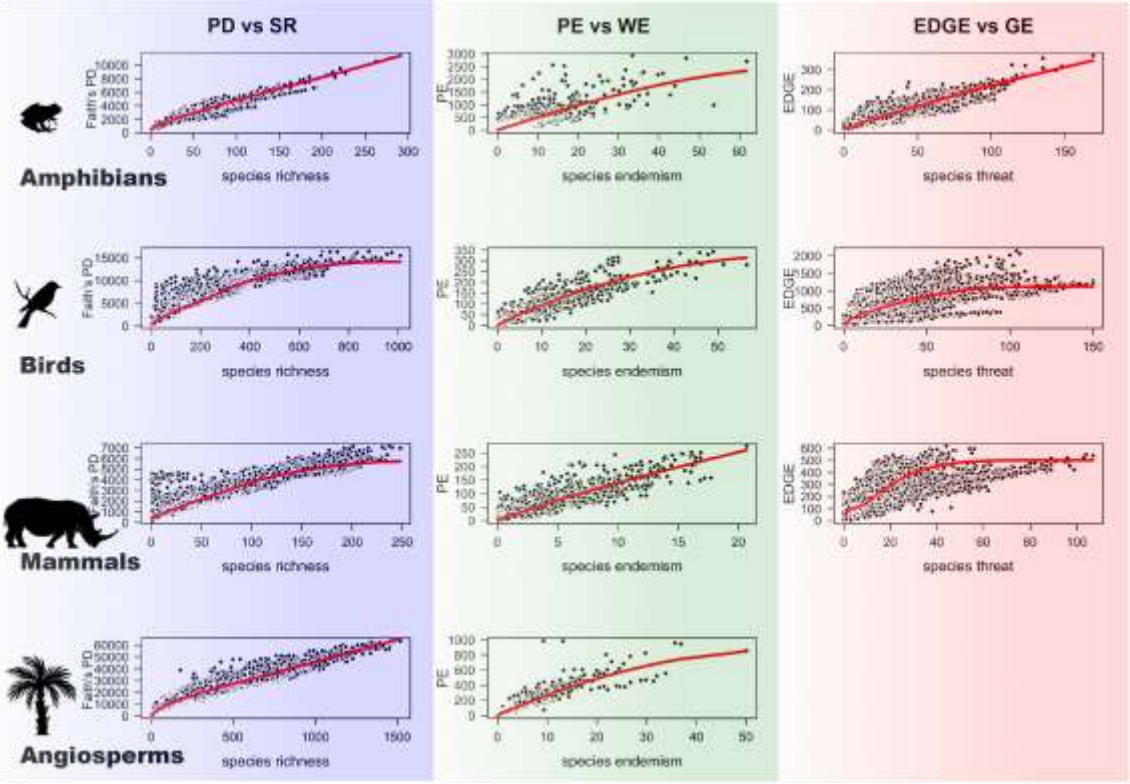

Fig. S10. Relationships among phylogenetic indices and their species-level variants across 1° × 1° grid cells for amphibians, birds, mammals and angiosperms. The red lines were fitted using loess regression of phylogenetic indices against species-level metrics. PD = Faith's phylogenetic diversity, SR = species richness (GR, genus richness for angiosperms), PE = phylogenetic endemism, EDGE = evolutionary distinctiveness and global endangerment, GE = global endangerment (species threat). EDGE was not computed for angiosperms because of lack of information on IUCN threat categories.

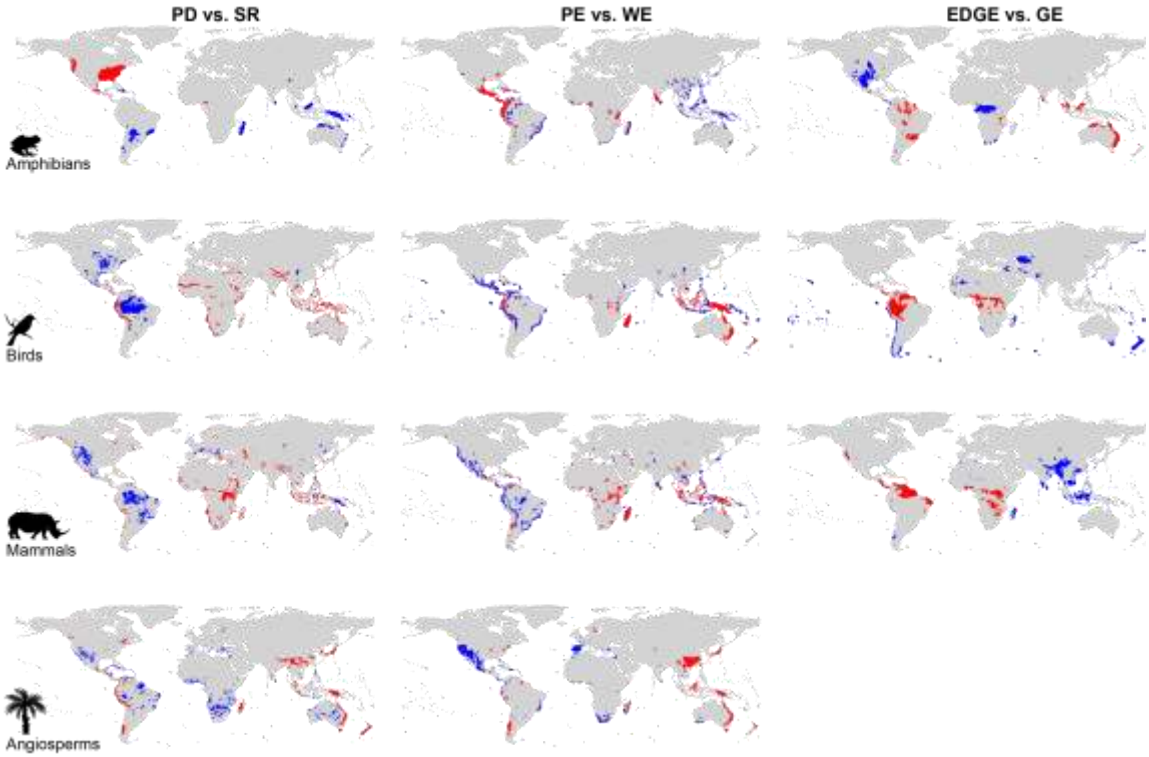

Fig. S11. Concentrations of positive residuals (hotspots: red) and negative residuals (coldspots: blue) from a regression model of PD vs SR, PE vs WE and EDGE vs GE for each taxonomic group. The hotspots and coldspots represent the top and bottom 2.5% of residuals respectively. PD = phylogenetic diversity; PE = phylogenetic endemism; EDGE = evolutionary distinctiveness and global endangerment; GE = global endangerment; SR = species richness; WE = weighted endemism. The maps are in Behrmann projection. EDGE was not computed for angiosperms because of lack of information on IUCN threat categories.

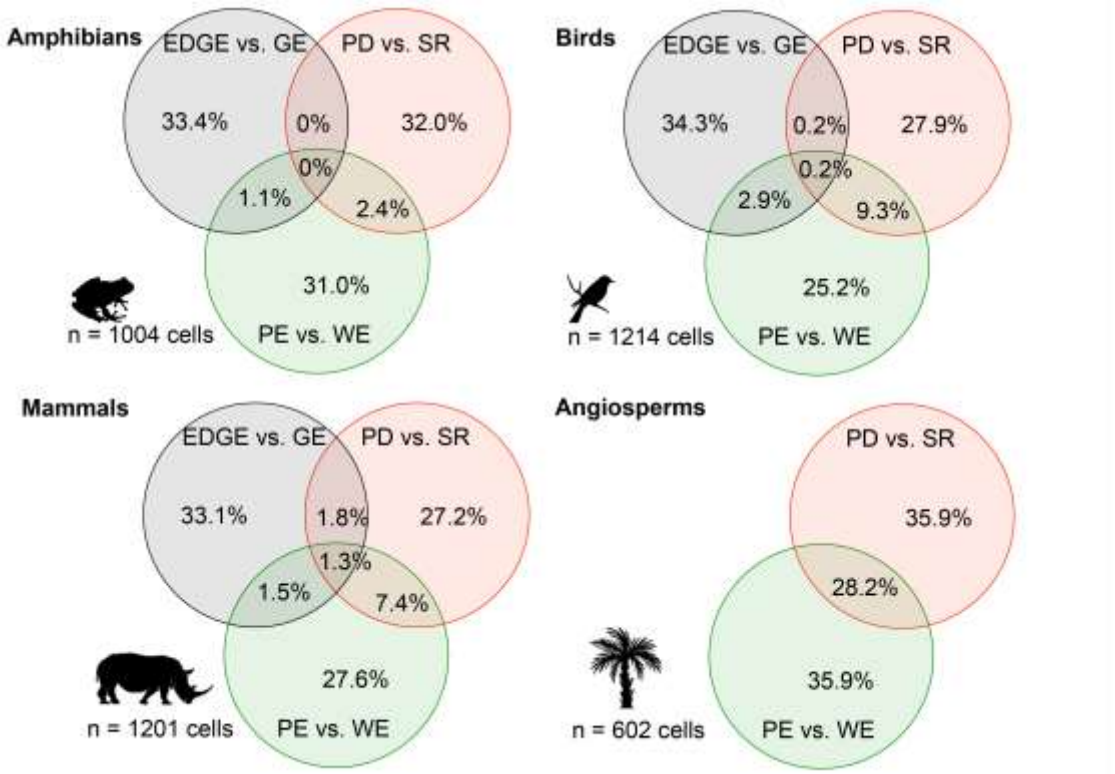

Fig. S12. Spatial congruence among hotspots of residuals from a LOESS regression model of PD vs. SR, PE vs. WE and EDGE vs. GE for each taxonomic group. The hotspots comprise the top 2.5% of residuals. PD = phylogenetic diversity; PE = phylogenetic endemism; EDGE = evolutionary distinctiveness and global endangerment; GE = global endangerment; SR = species richness (GR, genus richness for angiosperms); WE = weighted endemism. The values in Venn diagrams are the percentages of total number of hotspot grid cells (top 2.5% quantiles) covered by all metrics combined together, with the middle values representing grid cells shared by all three metrics, and the others are grid cells unique to each metric. EDGE was not computed for angiosperms because of lack of information on IUCN threat categories.

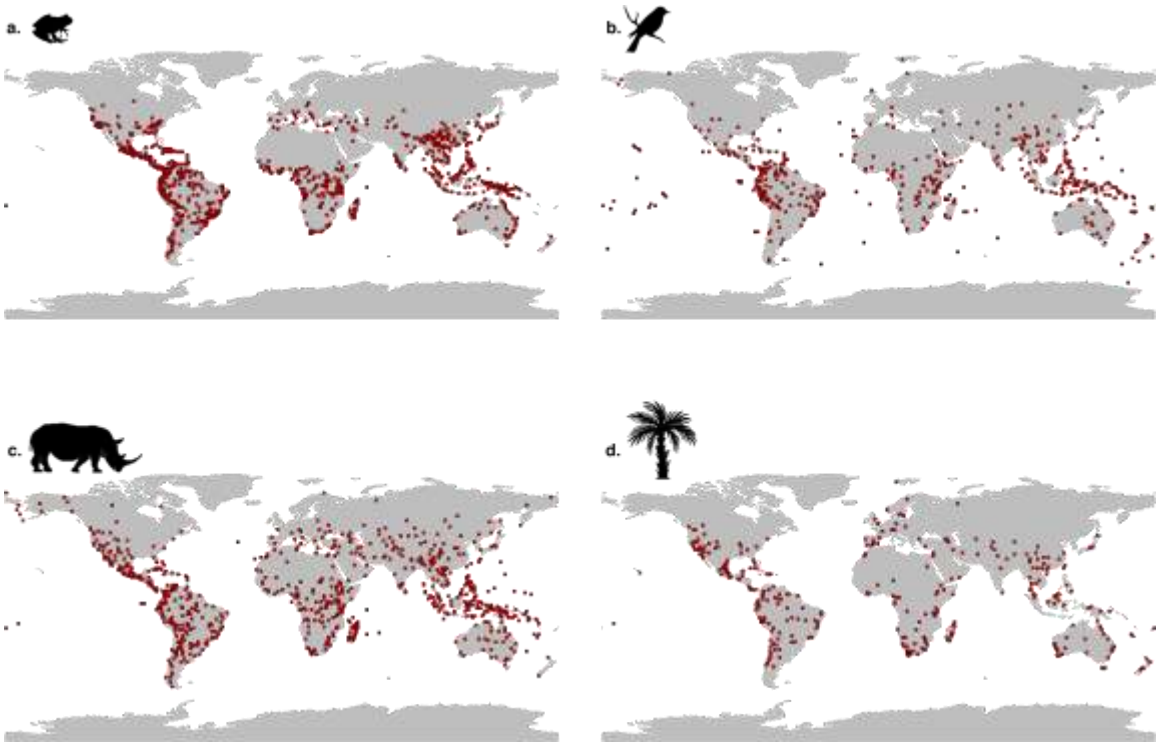

Fig. S13. Distribution of grid cells chosen by the PD-complementarity greedy algorithm that fully represents phylogenetic branch lengths in as few grid cells as possible. (a) Amphibians, (b) Birds, (c) Mammals, and (d) Angiosperms.

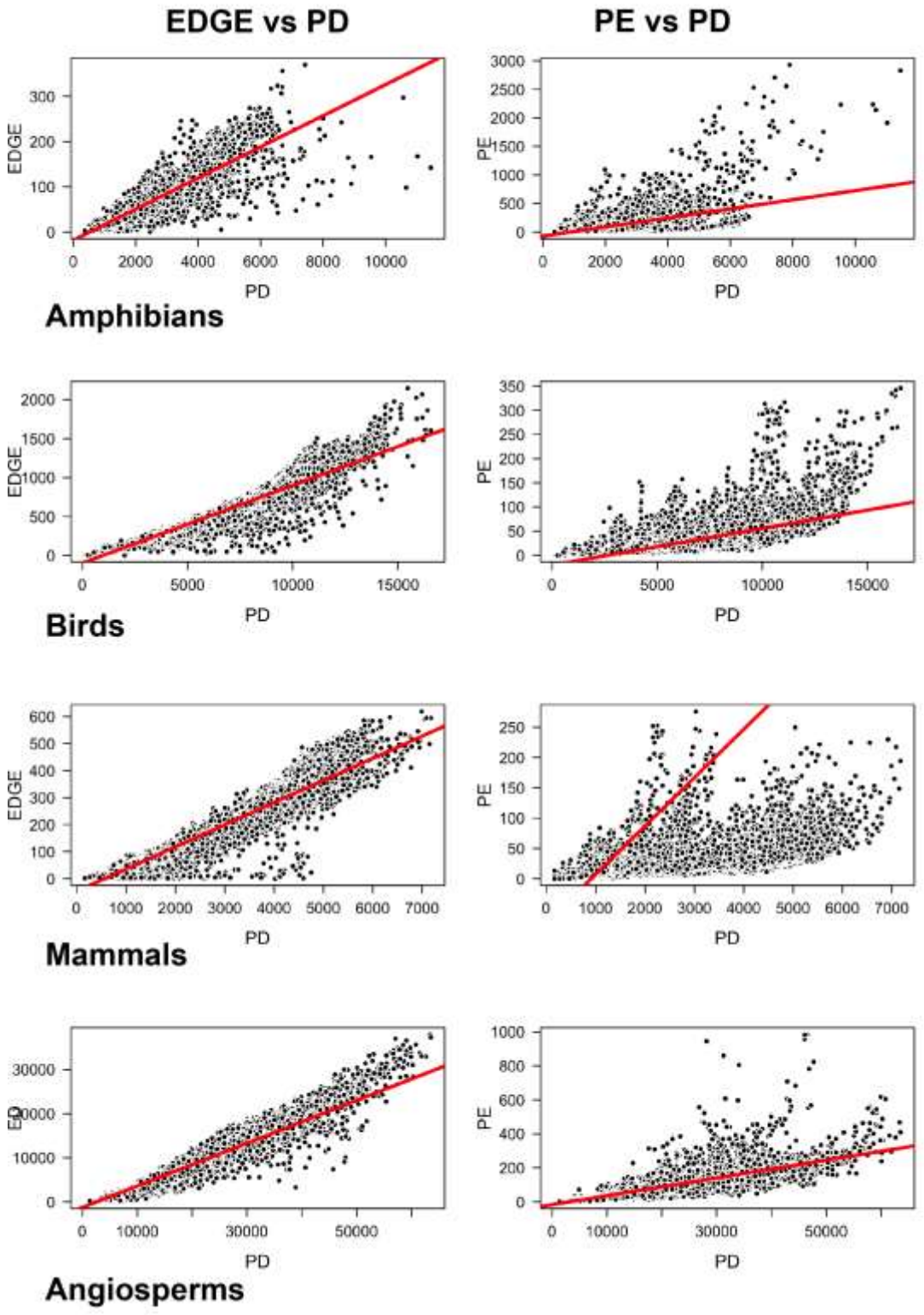

Fig. S14. Relationship of EDGE vs PD and PE vs PD for each taxonomic group to demonstrate the additional gains provided by PE and EDGE.